New insights into Kilauea's volcano dynmaics brought by large-scale relative relocation of microearthquakes.

Jean-Luc Got, P. Okubo

JOURNAL OF GEOPHYSICAL RESEARCH, VOL. 108, NO. B7, 2337, doi:10.1029/2002JB002060, 2003

New insights into Kilauea's volcano dynamics brought by large-scale relative relocation of microearthquakes

Jean-Luc Got
Laboratoire de Géophysique Interne et Tectonophysique, Université de Savoie, Le Bourget-du-Lac, France

Paul Okubo
Hawaiian Volcano Observatory, U.S. Geological Survey, Hawaii National Park, Hawaii, USA

Received 2 July 2002; revised 21 February 2003; accepted 17 March 2003; published 15 July 2003.

[1] We investigated the microseismicity recorded in an active volcano to infer information concerning the volcano structure and long-term dynamics, by using relative relocations and focal mechanisms of microearthquakes. There were 32,000 earthquakes of the Mauna Loa and Kilauea volcanoes recorded by more than eight stations of the Hawaiian Volcano Observatory seismic network between 1988 and 1999. We studied 17,000 of these events and relocated more than 70%, with an accuracy ranging from 10 to 500 m. About 75% of these relocated events are located in the vicinity of subhorizontal decollement planes, at a depth of 8–11 km. However, the striking features revealed by these relocation results are steep southeast dipping fault planes working as reverse faults, clearly located below the decollement plane and which intersect it. If this decollement plane coincides with the pre-Mauna Loa seafloor, as hypothesized by numerous authors, such reverse faults rupture the pre-Mauna Loa oceanic crust. The weight of the volcano and pressure in the magma storage system are possible causes of these ruptures, fully compatible with the local stress tensor computed by *Gillard et al.* [1996]. Reverse faults are suspected of producing scarps revealed by kilometer-long horizontal slip-perpendicular lineations along the decollement surface and therefore large-scale roughness, asperities, and normal stress variations. These are capable of generating stick-slip, large–magnitude earthquakes, the spatial microseismic pattern observed in the south flank of Kilauea volcano, and Hilina-type instabilities. Rupture intersecting the decollement surface, causing its large-scale roughness, may be an important parameter controlling the growth of Hawaiian volcanoes. *INDEX TERMS:* 7209 Seismology: Earthquake dynamics and mechanics; 7230 Seismology: Seismicity and seismotectonics; 7280 Seismology: Volcano seismology (8419); 8015 Structural Geology: Local crustal structure; 8020 Structural Geology: Mechanics; *KEYWORDS:* double difference, multiplet, earthquake, Kilauea, Hawaii, seismology, flank instabilities

Citation: Got, J.-L., and P. Okubo, New insights into Kilauea's volcano dynamics brought by large-scale relative relocation of microearthquakes, *J. Geophys. Res.*, *108*(B7), 2337, doi:10.1029/2002JB002060, 2003.

1. Introduction

[2] Hawaiian volcanoes share several typical features. Most of them show calderas at the summit and long rift zones, erupting magma and limiting the upper part of their flanks. Active volcanoes of the Hawaiian Islands, like Mauna Loa and Kilauea, show that these flanks are moving horizontally. In many active or ancient Hawaiian volcanoes, huge fault scarps or landslides have been evidenced along their flanks. Reproduction of these features across the volcanoes of the Hawaiian ridge shows that they may be caused by a common mechanical process, acting during at least the final stages of growth of these volcanoes. Studying seismicity occurring inside edifices of Hawaiian volcanoes may therefore help to understand how they grow. Early focal mechanism studies of the Kalapana (1975, M_s = 7.2) earthquake and its aftershocks [*Ando*, 1979; *Furumoto and Kovach*, 1979; *Crosson and Endo*, 1981, 1982; *Bryan and Johnson*, 1991] showed that most of the deformation of the south flank of Kilauea could be due to one or more 6–9 km deep subhorizontal planes. This hypothesis agrees with the analysis of geodetical measurements of the southward (N160° to 180°) displacement of the Kilauea south flank [e.g., *Swanson et al.*, 1976; *Lipman et al.*, 1985]. A decollement plane has been hypothesized by numerous authors to coincide with the top of the pre-Mauna Loa oceanic crust (Figure 1; hereinafter referred to as "the oceanic crust"), based on seismic refraction measurements by *Hill* [1969], *Zucca and Hill* [1980], and *Zucca et al.* [1982] [see also *Hill and Zucca*, 1987]. This interface is found by these authors to be north

0148-0227/03/2002JB002060$09.00

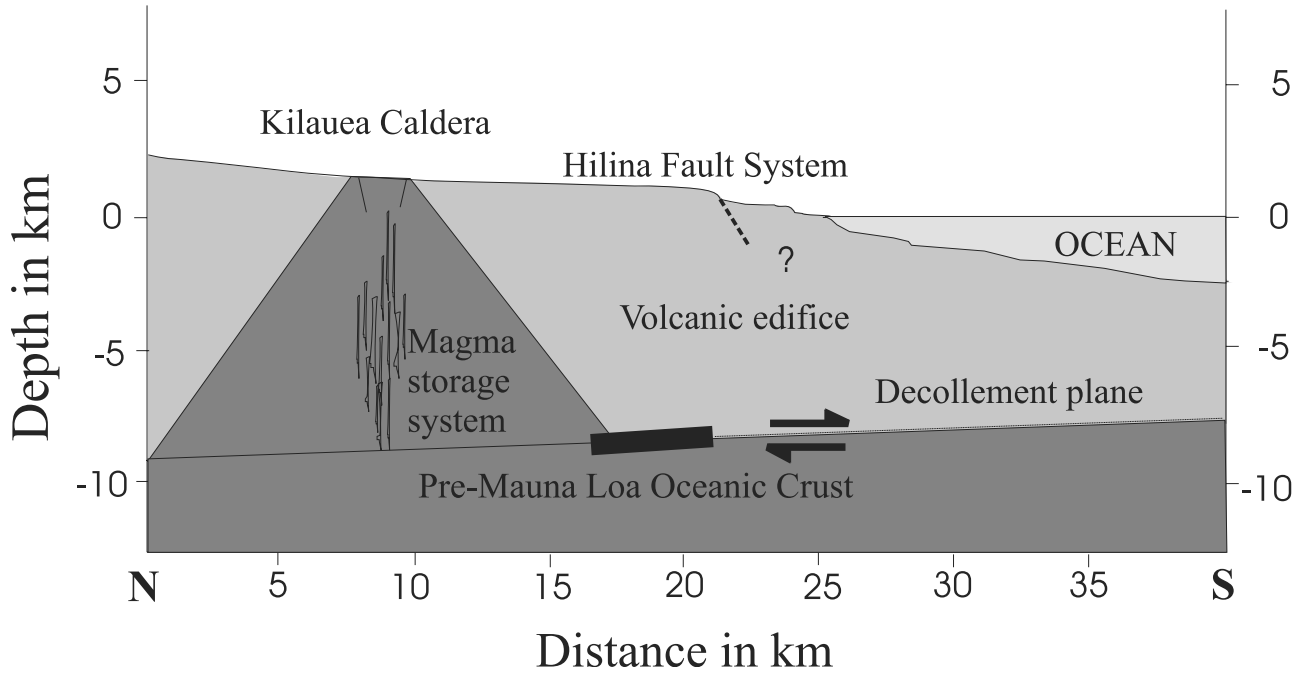

Figure 1. Schematic cross section showing the main features of Kilauea volcano. Crustal structure is from *Zucca and Hill* [1980], and decollement plane is from *Lipman et al.* [1985]. The seismogenic part of the decollement plane is indicated with a bold line; the aseismic part is indicated with a dashed line.

dipping below the south flank of Kilauea, with the northward dip interpreted as being due to the depletion of the crust under the load of the volcanic edifices [*Thurber and Gripp*, 1988]. *Dieterich* [1988] shows that the topographic slope of the volcano could be controlled by the apparent friction coefficient of such a north dipping decollement plane. *Got et al.* [1994] showed that most of the vertical dispersion in the absolute locations of the earthquakes recorded in the south flank of Kilauea was due to location error and that a significant proportion (∼25%) of the hypocenters collapsed into a single gently north dipping fault plane located at a depth of 8–9 km. In a very detailed and extensive study of focal mechanisms of earthquakes occurring from 1972 to 1992, *Gillard et al.* [1996] investigated the state of stress inside Kilauea volcano. They revealed that the faulting process was complex, comprising notably a large proportion (up to 80%) of reverse faulting, and not only decollement events. Such complexity was already suspected by *Bryan* [1992]. *Gillard et al.* [1996] show that faulting and the inferred state of stress were subject to spatiotemporal changes related to the intrusive and eruptive history of the volcano.

[3] Although these studies brought more and more light on the mechanical processes at work in active Hawaiian volcanoes, they do not allow us to understand fully how these volcanoes grow. In particular, although *Lipman et al.* [1985] identify the boundary between the upper and the lower parts of the south flank as a major structural feature of the volcano, not one of these studies could explain the striking distribution of the seismicity along the decollement plane nor the systematic existence of Hilina-type gravitational instabilities in Hawaiian volcanoes, and the location of reverse faulting was not clear in the edifice. In this study our aim is to go further in the understanding of the mechanical processes working during the growth of Hawaiian volcanoes by imaging, as accurately and extensively as possible, the seismogenic structure using an earthquake relative relocation method.

2. Data

[4] The data are 32,000 short-period seismograms from microearthquakes recorded from 1988 to 1999 by the Hawaiian Volcano Observatory (HVO) seismic network, composed of ∼50 short-period telemetered stations which operated during this period (Figure 2). Seismograms were digitized by the CUSP system at a rate of 100 samples per second and retrieved directly from the local CUSP database. Events for which arrival times were picked at eight stations at least were selected over a wide area (Figure 2) including Mauna Loa and Kilauea volcanoes, without using a computed magnitude or depth criterion. This selection of events exhibits statistical properties (Figure 3) representative of the total recorded seismicity in Hawaii. Both the catalog and the selection seem to be complete down to magnitude 1.5. We decided to limit this study to tectonic earthquakes; therefore earthquakes occurring in Kilauea caldera and rift zone roots, directly related to magma transfer during intrusion or to eruption episodes have been discarded from this selection using a simple geographical criterion. East rift zone similar earthquakes have been studied by *Gillard et al.* [1996] and long-period (LP) volcanic events of the caldera are studied by J. Battaglia (Relative locations of volcanic LP events of the Kilauea caldera, Hawaii, submitted to *Journal of Geophysical Research*, 2003). Events related to the deep magmatic

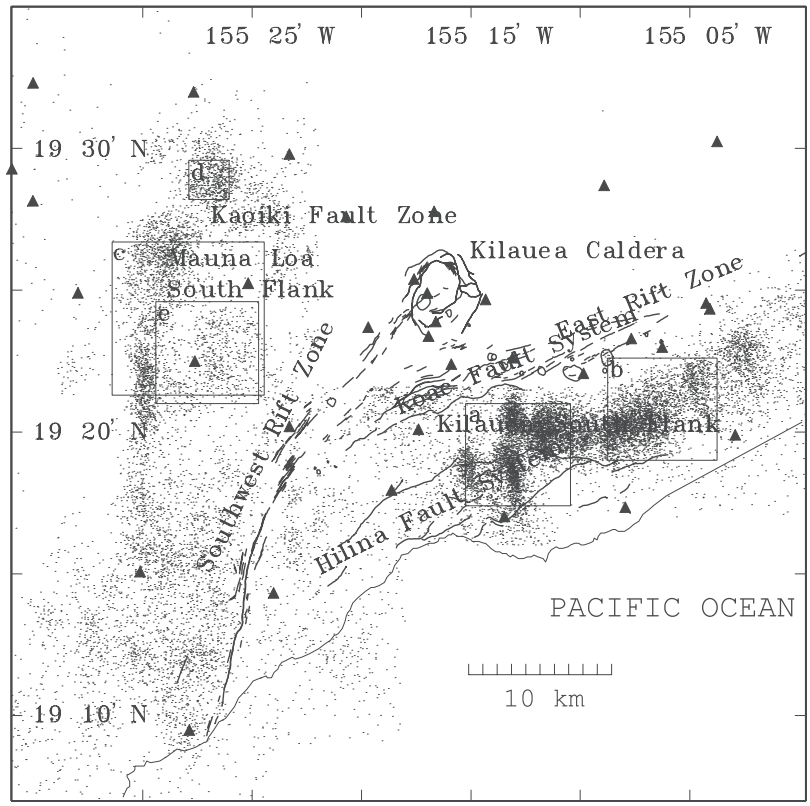

Figure 2. Map of Kilauea and adjacent part of Mauna Loa volcanoes, Hawaii, showing rift zones, fault systems, craters, epicenters of microearthquakes used in this study (dots), and seismic stations of the HVO seismic network (solid triangles). Boxes show the limits of the maps of the relocated events.

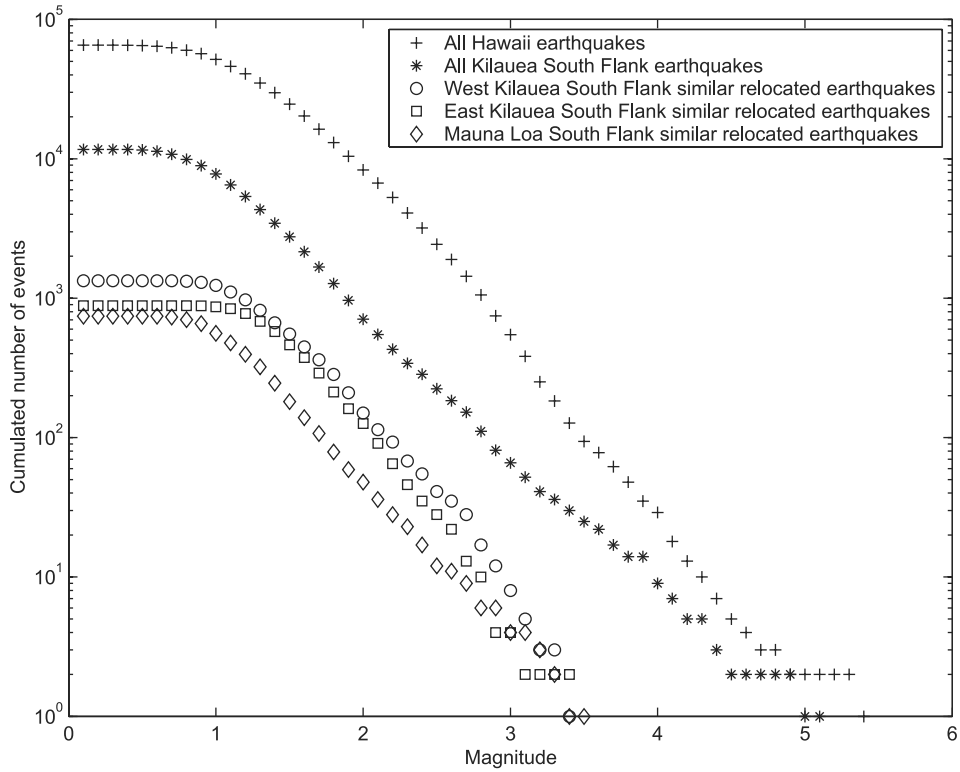

Figure 3. Cumulated number of events as a function of magnitude for various sets of seismic events recorded by the HVO seismic network.

system are studied by *Wolfe et al.* [2003]. Seventeen thousand events were finally used in this study.

3. Method

[5] Mauna Loa and Kilauea volcanoes are very heterogeneous structures and consequently exhibit high variability in the seismic velocity distribution at depth [*Okubo et al.*, 1997; *Haslinger et al.*, 2001]. One-dimensional (1-D) velocity models lead to a poor approximation of the medium and therefore to strong uncertainties in absolute locations. However, seismicity is very dense in many parts of these volcanoes. Such a density allows a natural linearization of the relative relocation problem, and therefore makes relative relocation less sensitive than absolute locations to the variability of the medium. Use of large sets of neighboring events to perform such relative relocation is now common [e.g., *Got et al.*, 1994; *Rubin et al.*, 1999; *Waldhauser et al.*, 1999; *Waldhauser and Ellsworth*, 2000] and has led to high-precision hypocenter determination. In this study we use the simple linear approach presented by *Got et al.* [1994] to massively determine the relative positions of neighboring earthquakes. Assuming the source-receiver distance is large compared to the average interevent distance, we consider that the time delay Δt_{ij}^k between traces recorded for two different but neighboring events i and j at the same station k is linearly related to the source relative position vector:

$$\Delta t_{ij}^k = \Delta t_{\text{orij}} + \mathbf{r}_{ij}\mathbf{s}^k = \Delta t_{\text{orij}} + x_{ij}s_x^k + y_{ij}s_y^k + z_{ij}s_z^k, \qquad (1)$$

where $\mathbf{s}_k = (s_x^k, s_y^k, s_z^k)^T$ is the slowness vector for the station k, $\mathbf{r}_{ij} = (x_{ij}, y_{ij}, z_{ij})^T$ is the source relative position vector for the (i,j) event pair, and Δt_{orij} is the origin time difference for the same event pair. In this study, $\mathbf{s}_k$ is determined from the 1-D P wave velocity model used as an initial model in the inversion leading to the tomographic model of Mauna Loa and Kilauea volcanoes presented by *Okubo et al.* [1997]. Equation (1) can therefore be formulated as an inverse problem in which the parameters of the model are $\mathbf{m} = (x_{ij}, y_{ij}, z_{ij}, \Delta t_{\text{orij}})^T$:

$$\mathbf{Gm} = \mathbf{d}, \qquad (2)$$

where $\mathbf{G}$ is the matrix containing the $\mathbf{s}^k$ partial derivatives of Δt_{ij}^k relative to the unknown vector $\mathbf{m}$ and $\mathbf{d}$ is the data vector, containing the P wave time delays. It is solved in a least squares sense by using the normal equation inversion scheme:

$$\mathbf{m} = \left(\mathbf{G}^T\mathbf{C}_d^{-1}\mathbf{G}\right)^{-1}\mathbf{G}^T\mathbf{C}_d^{-1}\mathbf{d}, \qquad (3)$$

where $\mathbf{C}_d$ is the data covariance matrix, using the Cholesky decomposition of $\mathbf{G}^T{\mathbf{C}_d}^{-1}\mathbf{G}$. The use of sets of all possible and different event pairs leads such a system to be strongly overdetermined, improving accuracy of its least squares solution.

[6] Positions found in $\mathbf{m}$ are always known relative to the geometric center of the set of events to be relocated. Therefore, and for simplicity, we will use the term "relocation" instead of "relative relocation", unless the latter expression is really necessary.

[7] Relocation accuracy is dependent on the accuracy obtained in the determination of travel time delays. Similar earthquakes can be used to measure time delays with a subsample accuracy using a cross-spectral analysis [*Jenkins and Watts*, 1968]. This approach gives a typical accuracy ranging from 5 to 50 m horizontally and 10 to 100 m vertically, for relative positions. It provides a very detailed picture of the seismogenic structures and is primarily used in this study to relocate kernels of very similar events.

[8] As the linearization of the relative relocation problem only works for events closer than a fraction of the source-receiver distance, the complete relocation of similar events is performed on a large extent using an iterative algorithm. The initial stage consists in the relative relocation of a kernel of highly similar events as described previously. To limit error propagation, each iteration allows the relocation of one event relative to the already relocated events from the modified Cholesky solution of the normal equations:

$$\mathbf{m_2} = \mathbf{H_2}^{-1}\left(\mathbf{G}^T\mathbf{C}_{\text{d}}^{-1}\mathbf{d} - \mathbf{H_1}\mathbf{m_1}\right),$$

where $\mathbf{H_1} = (\mathbf{G}^T{\mathbf{C}_d}^{-1}\mathbf{G})_\mathbf{1}$ and $\mathbf{H_2} = (\mathbf{G}^T{\mathbf{C}_d}^{-1}\mathbf{G})_\mathbf{2}$ correspond to the events already relocated and to be relocated, respectively, and $\mathbf{m_1}$ is the vector containing the already computed relative positions and origin time differences.

[9] The event to be relocated is the one which exhibits the highest coherency with a given minimum set of events (typically 20) belonging to the already relocated multiplet. At each step, a local mean slowness vector is recomputed from this coherent set of events and the new event is relocated relatively to this coherent set. This iterative approach leads therefore to a progressive relaxing of the coherency between events. The iterative process stops when no other event exhibits an average coherency greater than a given threshold (set in this study to 80%) with a minimum set of already relocated events (set to 20).

[10] Events sharing similar waveforms with their nearest neighbors offer the advantage of applying a local spatial filtering along the focal mechanisms and therefore of displaying a clear and smoothed picture of the fault surface. However, information is contained in events which are not relocated using this similarity criterion, as the former relocation process removes a part of the complexity of the stress field in the vicinity of the fault surface. It is therefore of interest to complete the relocation with nonsimilar events while keeping the best possible accuracy, or merely to estimate the statistical distribution and density of nonsimilar earthquakes in the vicinity of already relocated similar earthquakes. To that aim, the iterative process described for relocating similar earthquakes is extended by using travel time differences computed from phase pickings instead of time delay computed from cross-spectral analysis. To fulfill the common ray hypothesis and remain in the frame of our fully linear approach, we restrict these calculations to events neighboring already relocated events. This closeness criterion was previously fulfilled via the use of a more restrictive coherency criterion. To retrieve nonsimilar neighboring pairs of

events, we compute the correlation coefficient between the travel time series corresponding to both events, recording stations being ordered in the same way for both events. It provides an approximate method to constitute pairs of neighboring events: such events have a strong correlation coefficient, although picking errors tend to lower it. For this reason a set of events having a strong correlation coefficient is an incomplete set of neighboring events. This set will be completed by relaxing the correlation coefficient: it is therefore used in the iterative algorithm in the place of the coherency coefficient. The set of already relocated similar events is used to initialize the process; at each iteration, the event chosen to be relocated exhibits the highest correlation coefficient with a set of already relocated events. Correlation between events is therefore progressively relaxed; the threshold used to stop iteration is 99%, corresponding to an average distance of 3 km.

4. Results

4.1. Accuracy

[11] Sources of uncertainty in relative relocation include time delay and velocity model uncertainty. Cross-spectral estimation of time delays for well-coherent earthquake pairs leads to an average uncertainty lower than 5 ms. Uncertainty in travel time difference computed from hand pickings is estimated in this study by comparison with the corresponding value of time delay estimated from cross-spectral analysis, for highly coherent earthquake pairs. Statistical distribution and standard deviation of the differences between both series (comprising up to 1.2 million time delays) allow the accuracy of travel time difference determined from hand pickings to be estimated to be $\sim$70 ms, leading therefore to an average arrival time picking accuracy of 50 ms.

[12] Taking into account velocity model uncertainty in relative relocation uncertainty entails the use of Monte Carlo methods. Such calculations, performed with an average uncertainty of 5° in azimuth and takeoff angles and the above estimated uncertainty for time delays, lead to an average uncertainty in relative positions of 30 m horizontally, 50 m vertically when cross-spectral time delay data are used, whereas it is 250 m horizontally, 400 m vertically when arrival time picking difference data are used.

4.2. Relocations

[13] About 4000 events have been relocated from *P* wave cross-spectral time delays using a coherency threshold of 80%, an additional 8000 being relocated using arrival time picking differences, most of them in the south flanks of Kilauea and Mauna Loa (Figures 4–6). Relocated seismicity represents up to 90% of the total seismicity in the western south flank of Kilauea, 70% in the eastern, and $\sim$50% in Mauna Loa southeast flank. Relocated similar earthquakes represent only 30% of the total seismicity in the western south flank of Kilauea and $\sim$25% of the total seismicity of Kilauea and Mauna Loa volcanoes, a relatively low percentage as compared to that observed (75%) in some parts of the San Andreas and Calaveras faults [*Rubin et al.*, 1999]. Figure 3 shows that the relocation process preserves the Gutenberg-Richter scaling law but generates an intrinsic upper magnitude cutoff. This cutoff is controlled by the probability of getting similar events of a given magnitude during the observation duration and is therefore related to the observation duration, the seismicity rate, and the individual event magnitude distribution.

[14] Figure 4 shows relocations realized using time delays computed from cross-spectral analysis, with a coherency greater than 80%. Seismicity appears to be more clustered in the western part of the south flank of Kilauea (Figure 4a) than in the eastern part (Figure 4b) and in the southeast flank of Mauna Loa (Figure 4c). In the following, we will try to describe this clustering more clearly by using the terms ''plane'' and ''lineation'' to describe planar and linear sets of relocated hypocenters, respectively. In this way, structural information can be extracted from the more frequent directions existing between neighboring hypocenters. Measurements of strike and dip of these geometrical elements have been made using least squares fits of the corresponding sets of relocated hypocenters. In the western part of Kilauea (Figure 4a), this study allows the retrieval of the 8- to 9-km-deep subhorizontal plane evidenced by *Got et al.* [1994]. More accurately, this subhorizontal set of relocated hypocenters consists of one N55°, 22°N northern plane (labeled a in Figure 4a) and one N85°, 20°N southern plane (labeled b in Figure 4a), and a set of N160° horizontal lineations (labeled c in Figure 4a). Seismicity inside the planes appears to be strongly clustered, and in some places, structured in lineations rather than randomly distributed. Seismicity relocated in the northern plane a consists of two (one N45° and one N60°) 1-km-long horizontal lineations, and one N145°, 20°N at the NE end of the two N45°–N60° lineations, forming a characteristic corner. Seismicity relocated in the southern plane b comprises a 1-km-long N90° horizontal lineation, and numerous clusters. A significant number of these clusters are aligned following two nearly perpendicular N60° and N145° directions, delimiting roughly a 1 km^2 squared area with characteristic corners, most of this area being empty of events.

[15] In the southern part of the area covered by Figure 4a, we find one N70°, 65°S dipping plane (labeled d in Figure 4a), covering an area larger than 2 km^2. It consists mainly of one cluster, elongated in the N160°, 65°S direction. The top of this plane corresponds to the depth of the N85°, 20°N plane b at that place and identifies with a 1-km-long N70° horizontal lineation. Two other smaller earthquake clusters also define N70°, 65°S planes at the southern end of the major southern dipping plane d. The southernmost of them comprises a 400 m long N160°, 65°S lineation.

[16] In the eastern part of the Kilauea south flank (Figure 4b), most of the relocated hypocenters define a subhorizontal N50° striking, 20°N dipping plane and two N50°–60° striking, 50°S dipping planes. We therefore find again structures analogous to those evidenced in the western part of the Kilauea south flank.

[17] In the southern part of the southeast flank of Mauna Loa (Figures 4c–5c), relocated hypocenters clearly evidence a 10 to 11 km deep subhorizontal plane covering an area larger than 25 km^2. The southern part of this plane is horizontal, the northern is N85° striking, 15°N dipping. However, an interesting and new feature is the 5 to 7 km deep subvertical N45° plane (Figure 4e), which covers a 10 km^2 area and represents a structural direction not found in the Kilauea south flank. A similar direction is found in

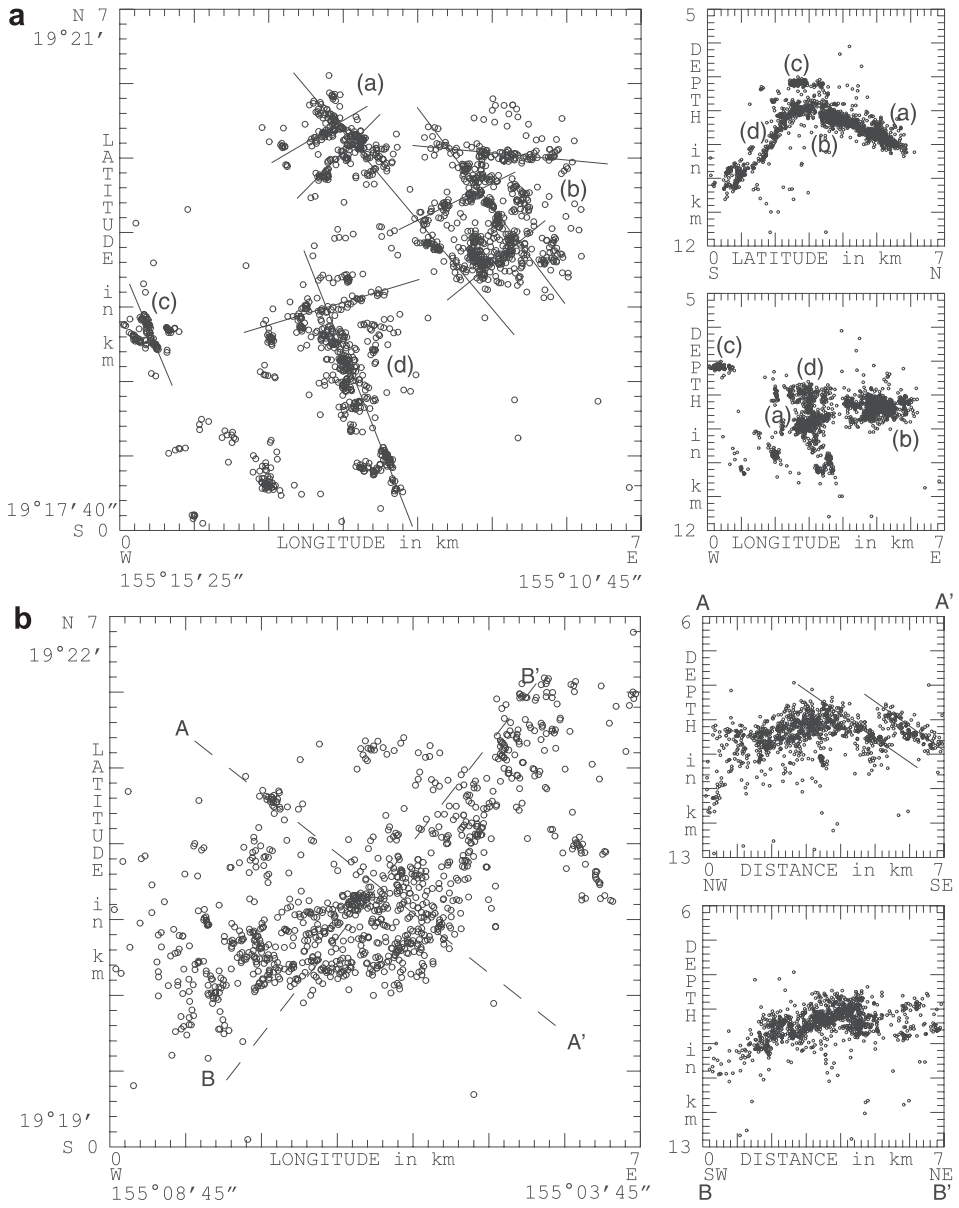

Figure 4. (left) Map and (right) vertical cross sections of the seismicity relocated using time delays computed from cross-spectral analysis. Subplots fit the boxes indicated Figure 2. There are 1702 (Figure 4a), 1142 (Figure 4b), 784 (Figure 4c), 154 (Figure 4d), and 33 (Figure 4e) events relocated. Each cross section is a projection along a vertical plane of the hypocenters comprised in the corresponding box. Lines indicate structural features described in the text. Directions of the vertical cross sections are indicated in the maps by dashed lines when they are neither N-S nor E-W.

the northern part of the Mauna Loa SE flank, where relocated hypocenters define a family of subvertical N30° striking planes (Figure 4d).

[18] Relocating new nonsimilar or poorly similar events (<80% coherency) using the kernel of already relocated similar events and travel time differences with a limitation on the relative location RMS of 0.03 s (Figure 5) leads to the addition of ~1000 events without there being a qualitative change (at the scale used) in the relocation image, whereas it does tend to obscure the image. It proves that a significant number of nonsimilar or poorly similar events are located in the vicinity of the structures evidenced by relative relocation of similar earthquakes. However, this technique, applied to the dense set of vertical strike-slip faults evidenced in the northern part of the southeast of Mauna Loa (Figure 4d), reveals a dense 3-km-diameter swarm, showing no significant structure: the structural information has been cancelled by the relocation error.

[19] Continuing the relocation process until the correlation coefficient is relaxed to 0.99 (corresponding to an interevent distance of ~3 km) and the RMS to 0.06 s allows the relocation of the seismicity in the western and the eastern sides (90% and 70%, respectively; Figure 6) of the south flank of Kilauea, without losing the large-scale information present in Figure 4. Most of the seismicity occurring in the south flank of Kilauea is therefore related to

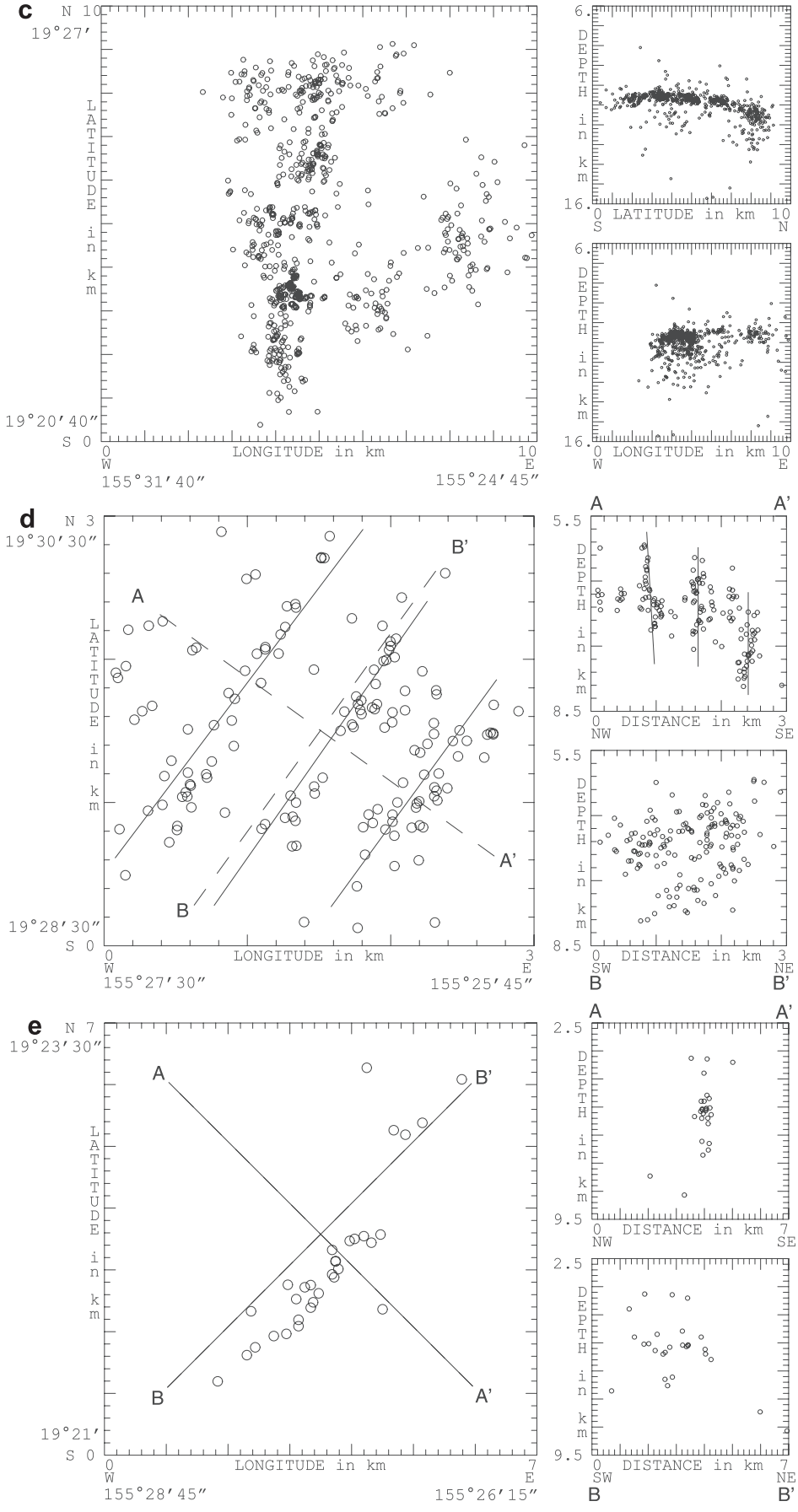

Figure 4. (continued)

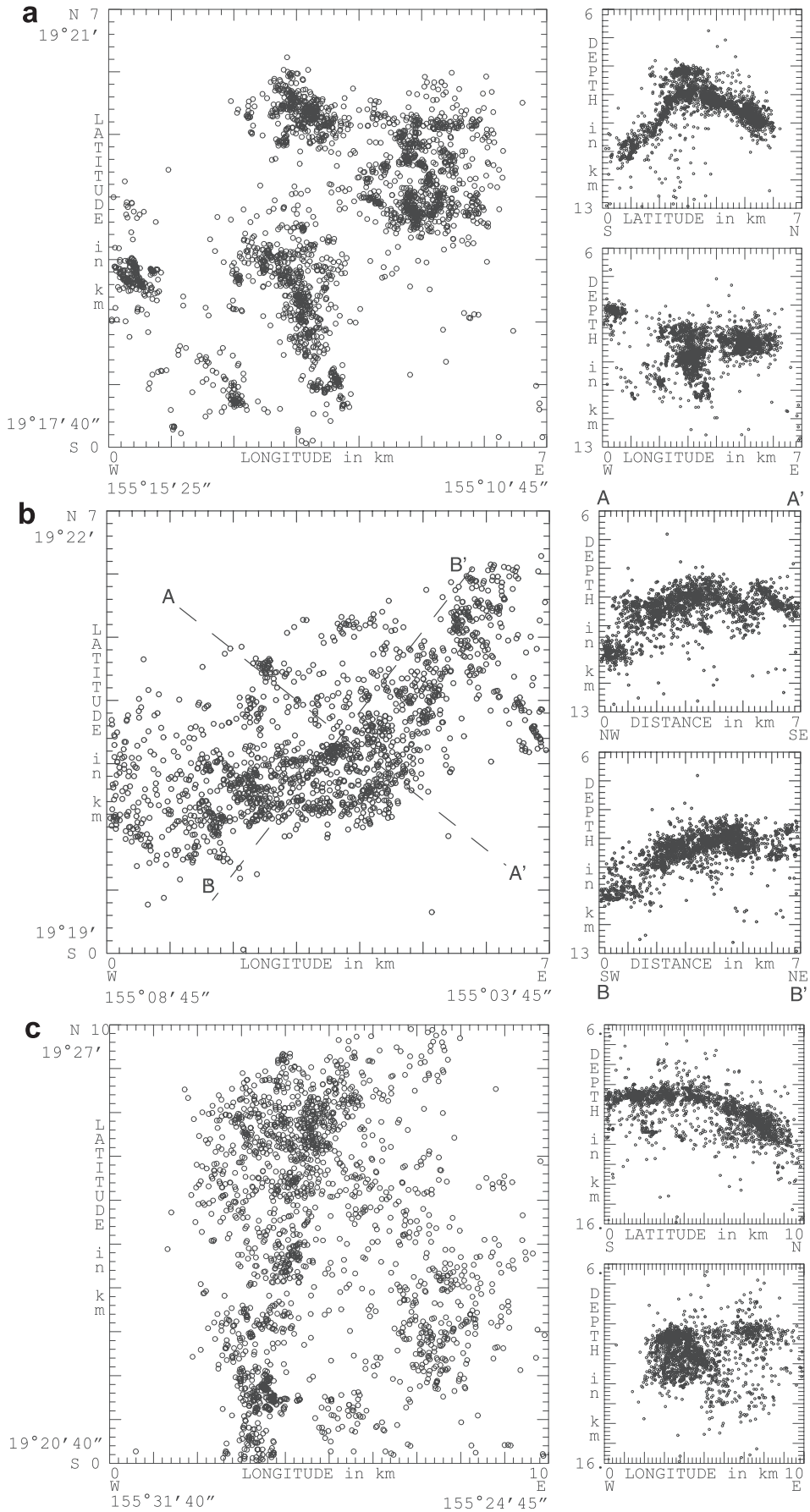
a
N 7
19°21′
LATITUDE in km
19°17′40″
S 0
0
W
LONGITUDE in km
7
E
155°15′25″
155°10′45″
6
DEPTH in km
13
0 LATITUDE in km 7
S
N
0 LONGITUDE in km 7
W
E
b
N 7
19°22′
A
B′
A′
B
19°19′
S 0
155°08′45″
155°03′45″
A
A′
0 DISTANCE in km 7
NW
SE
SW
NE
B
B′
c
N 10
19°27′
19°20′40″
S 0
10
155°31′40″
155°24′45″

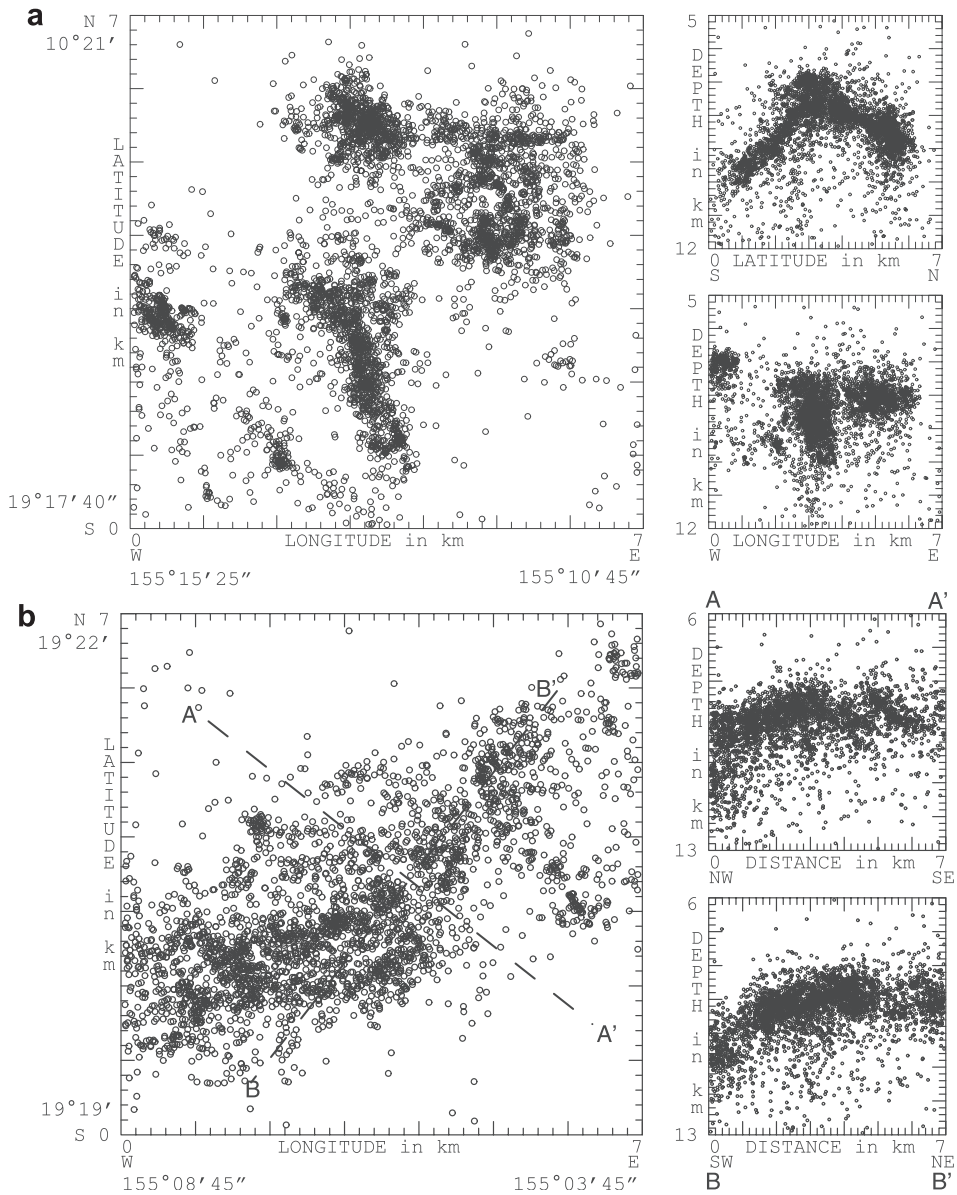

Figure 6. Same as Figure 5, RMS lower than 0.06 s with (a) 4953 of 5526 and (b) 4597 of 6543 events relocated.

the seismogenic structures already evidenced by relative relocation of similar events (Figures 4a and 4b).

5. Discussion

[20] Relocated events, similar or not, are strikingly condensed in the vicinity of some fault planes located in the south flanks of Kilauea and Mauna Loa. Figures 5c and 6 notably prove that most of the seismicity occurring in these flanks is related to the seismogenic structures evidenced by relocation of similar events. It does not mean that all events share the same focal mechanism, but it does mean that most of the deformation occurs within limited depth intervals. In the following, we will discuss thoroughly the consequences of this distribution of the deformation.

5.1. South Flank of Kilauea

[21] In the south flank region of Kilauea, 90% of the seismicity is located in the immediate vicinity of two major fault plane families. About 30% of them are located as similar earthquakes occurring on the fault plane itself, and 70% of them are located in the vicinity using travel time differences (Figures 4a, 4b, 5a, and 5b). It is not known to what extent the focal mechanisms of those earthquakes located using catalog travel time differences may differ from those of the similar earthquakes. In both of the western

Figure 5. (opposite) Same as Figure 4, for the seismicity relocated using Figures 4a–4c relocated swarms as kernels of similar events and travel time differences for nonsimilar events. Events are relocated with a RMS lower than 0.03 s with (a) 2621, (b) 2054, and (c) 2091 events relocated.

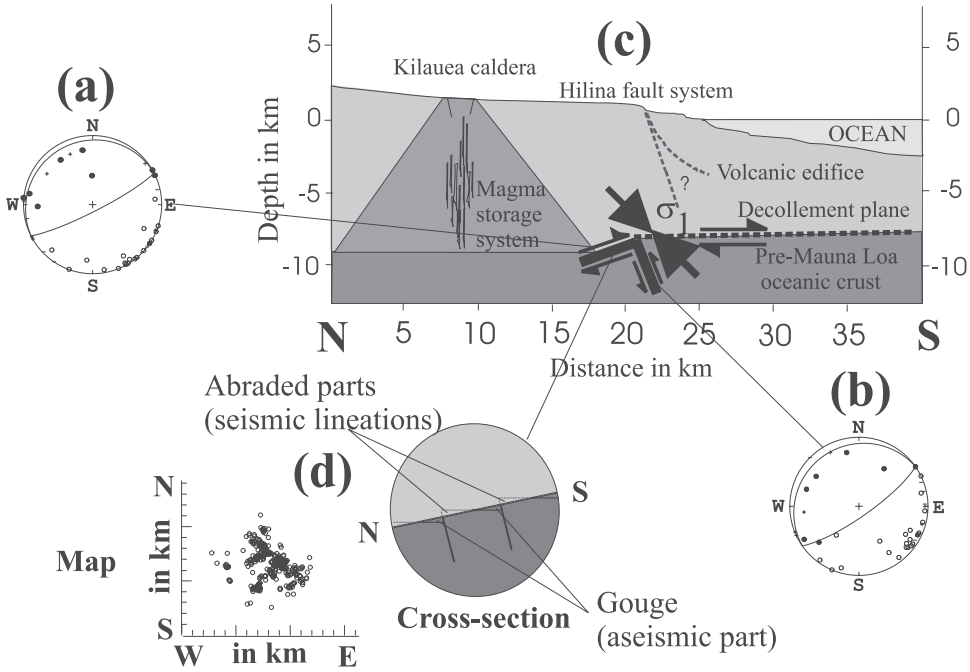

Figure 7. (a) Focal mechanism (lower hemisphere projection) of a $M_L \sim 3$ earthquake of the N55° striking plane of the decollement surface, leading to a N55°, 12°N solution. (b) Focal mechanism (lower hemisphere projection) of a $M_L \sim 3$ earthquake of the reverse fault plane, leading to a N63°, 82°S solution. (c) Schematic cross section showing the topography of Kilauea volcano, crustal structure from *Zucca and Hill* [1980], stress tensor from *Gillard et al.* [1996], Hilina fault system, the decollement plane, and geometrical features inferred from this study. The seismogenic part of the decollement plane and the reverse fault plane are indicated with a bold line, the aseismic part is indicated with a dashed line. (d) (left) Map of the N55° striking plane located in the northern part of the decollement plane (see Figure 4a plane a), showing N45° to 60° lineations, and (right) a schematic cross section showing a possible explanation for the slip-perpendicular seismic lineations and the steepening of the decollement plane.

(Figure 4a and 5a) and the eastern part (Figure 4b and 5b), relocations not only show a gently north dipping fault plane, similar to the fault plane already evidenced by *Got et al.* [1994] and hypothesized to allow the south flank to slip southward at the top of the oceanic crust, but also a family of N45 to 60° striking, 50 to 60°S dipping fault planes. A simple interpretation could link the latter fault parameters to the Hilina fault system. However, we will show in the next paragraph that both the focal mechanism and the depth of the inferred fault plane allow this explanation to be discarded.

5.1.1. Structural Implications and Coherence With the Local Stress Tensor

[22] It is at first surprising to relocate using waveform similarity, two structures whose orientations differ strongly. However, although the orientations differ, waveforms recorded by most of the seismic stations remain remarkably similar for neighboring events across the structures [see also *Kilb and Rubin*, 2002]. Focal mechanisms are almost identical for both decollement and steep south dipping fault planes (Figures 7a and 7b) and in good agreement with the planes inferred from relocations and show that they are perpendicular and working as reverse faults. A first conclusion is that the events located on the steep south dipping reverse fault plane are not directly related to the subjacent Hilina normal fault system. Relocations allow dips to be inferred, which are possibly averaged over multiple subparallel fault planes forming en échelon fault systems. Although they have to be compared with care to dips issued from focal mechanisms of individual ruptures of rock, we see that both dips share similar values close to 60°S. Steep south dipping reverse faults were already evidenced by numerous authors [e.g., *Gillard et al.*, 1996], and *Bryan* [1992] suspected them of triggering the slip of large areas along the decollement plane. It was however impossible to relate reverse faulting and decollement processes with certainty.

[23] The similarity of the waveforms through the fault planes leads to an accurate relative relocation of the reverse fault relative to the decollement plane. The reverse fault is clearly located below the decollement plane. In the hypothesis used in this discussion, following numerous authors [*Ando*, 1979; *Furumoto and Kovach*, 1979; *Crosson and Endo*, 1981, 1982; *Endo*, 1985; *Lipman et al.*, 1985; *Dieterich*, 1988; *Bryan and Johnson*, 1991; *Dieterich et al.*, 2000], that the 8- to 9-km-deep decollement plane lies at the top of the (pre-Mauna Loa) oceanic crust rather than within the volcanic edifice itself, then the reverse fault is located inside the oceanic crust. The understanding of a reverse fault in the crust at that place and in that context is, however, not straightforward. In a very detailed study of focal mechanism, faulting, stress and strain in the south flank of Kilauea, *Gillard et al.* [1996] showed that decollement, reverse and normal faults coexist in the south flank. However, they show that most M < 7 earthquakes in the south flank occurred along N40° striking, 60°S dipping

reverse faults, these earthquakes representing 80% of the total seismic moment of the south flank. This trend is especially true during periods where internal pressure, due to magma storage at a depth of ~5 km [*Delaney et al.*, 1990]), is increasing (e.g., 1972–1983). During this time the percentage of reverse faulting events is higher than decollement and normal ones [*Gillard et al.*, 1996]. Such a source of pressure adds to volcano weight, to induce a stress field with a largest principal stress σ_1 plunging at an average of 45° [*Gillard et al.*, 1996]. Taking the dip of σ_1 in the range [40°, 50°] and a value of the angle of internal friction in the range [30°, 50°] leads to dips in the range [60°, 80°] for crustal reverse faults, compatible with values inferred from earthquake focal mechanisms and relocations (Figure 7).

5.1.2. Consequences for Seismicity Pattern, Volcano-Seismic Cycle, and Volcano Growth

[24] Spatial distribution of microseismicity in the south flank of Kilauea may be related to reverse faulting. Indeed, stress induced by magma storage and setting in the rift zones provokes the slip along the steep reverse crustal faults and the decollement plane. Reverse faults clearly intersect, and therefore deform, the decollement surface. Scarps created by the work of steep reverse faults can on a small-scale produce rough lineations on the surface of the decollement plane, whose continuous abrasion may produce some slip-perpendicular alignments of hypocenters imaged by relative relocations (Figures 4a and 7). As observed on the map (Figure 2), seismicity in the south flank of Kilauea is limited to a narrow SW-NE band. Therefore seismogenic reverse crustal faults are limited to this band. Figures 4a and 4b show that the more active reverse faults in the period investigated are more external in the seismogenic structure. This fact could be interpreted as being due to the brittle response of the crust to the progressive growth of the volcano, acting as a very slow strain wave leaving the active volcanic rift: the (more) active reverse faults are therefore located close behind the strain wave front.

[25] Northward dip of the decollement plane inferred from relative relocations and focal mechanisms may also be itself related to reverse faulting. It is indeed N10°–20° and is actually clearly stronger (Figure 7c) than the 1–2° dip inferred from refraction measurements [e.g., *Zucca and Hill*, 1980] or computed from mechanical studies, taking into account the load of the volcano on an elastic plate [*Thurber and Gripp*, 1988]. Work of reverse faults intersecting the decollement plane may help to explain this relatively strong value of the dip (Figure 7d). Such a dip can be responsible for the uplift observed immediately south of the Koae fault system [*Fiske and Koyanagi*, 1968; *Swanson et al.*, 1976; *Lipman et al.*, 1985].

[26] As hypothesized above, it is likely that reverse faulting participates in the basal decollement deformation by creating and regenerating large-scale roughness. This process has probable consequences on the volcano-seismic cycle and earthquake magnitudes. Periodic regeneration of the roughness prevents the complete smoothing of the basal decollement surface. Such a smoothing would lead to creeping, as experienced by some segments of the San Andreas fault in northern California. Subvertical scarps of various scales can therefore lock the horizontal movement during periods of time, leading to the recording of less numerous decollement events than reverse events (see, for example, year 1974 of *Gillard et al.* [1996]), and quiescence [*Wyss et al.*, 1981]. *Wyss et al.* [1981] identified this region of the decollement plane as an asperity.

[27] In the short term, stress accumulates along the asperities of the decollement plane until the triggering of a large Kalapana-type decollement event. During this phase, both the rupture of large geometrical asperities and the conjugate work of decollement and crustal reverse faults may explain the magnitude of the largest decollement events: the possibility of the induction of large decollement events by small reverse events of the volcano has been already hypothesized by *Bryan* [1992]. The new image with reverse faults in the crust below the volcano edifice leads to hypothesize that crustal compartments between reverse faults may act on the base of the south flank as brake blocks controlled by magma pressure in the magma storage system and the long-term increase in weight of the volcano. Roughness of the basal decollement plane and changes in normal stress increase the probability of large decollement events. Once such large events occur, deflation, normal faulting and finally intrusions and eruptions take place in the East Rift and the Caldera. Studies by *Gillard et al.* [1996] and *Dieterich et al.* [2000], together with this study show that microseismicity of Kilauea's edifice, and especially statistics concerning the type of faulting, could therefore be used as a strain gauge and help to infer long-term pressure variations in the magmatic storage system and position in the seismo-volcanic cycle.

[28] On larger timescales, areas of the decollement plane may be locked by the work of crustal reverse faults. Such a process could limit the southward expansion of the volcano, favor the in-plane propagation of rifts, and control the flow rate of magma inside the rifts; *Dieterich* [1988] shows that the apparent coefficient of friction could control the average slope of the volcano. Large-scale roughness of the basal decollement plane could therefore be an important parameter controlling the growth, topography, deformation, and long-term eruptive dynamics of Hawaiian volcanoes, especially of their rifts.

5.1.3. Hilina Fault System

[29] Hilina large-scale instabilities occur in a dilatational quadrant of the pre Kalapana-type event stress field. The south flank of Kilauea slips on a subhorizontal decollement plane, whose parts have 10°–20° northward dips and act as asperities during this movement (Figure 7c). Compression is therefore expected upstream from the asperity and tension downstream. Such a phenomenon has been evidenced by geodetic measurements before the 1975 *M* 7.2 Kalapana earthquake [*Delaney et al*., 1992] and quoted by *Got et al.* [1994]. Tension downstream to the 10°–20° northward dipping fault plane can be responsible for the initiation of the Hilina instabilities. Notice that in that frame, Hilina instabilities originate from a deep process and are not initiated by gravity alone, although most of the deformation along the Hilina fault system occurs during Kalapana-type large decollement events [*Lipman et al.*, 1985] and is driven by gravity. Such a tensional origin for the Hilina instabilities may explain their size and help put constraints on the extent of their depth: tensional initiation at depth and more superficial gravitational coseismic movements could occur on two or more different, although related, rupture surfaces (Figure 7c).

Hilina-type instabilities could therefore be an indirect but superficial evidence of basal large-scale roughness and crustal reverse faulting in Hawaiian volcanoes. In the same way that an apparent coefficient of friction can explain the average (first order) value of the topographic slope [*Dieterich*, 1988], changes in the dip of the decollement plane could explain (second order) changes in the topographic slope.

[30] The Hilina fault system could be suspected of generating a significant part of the local microseismicity. One of the consequences of the location in the oceanic crust of the steep reverse fault plane is that <10% of the recorded seismicity occurs in the deforming south flank without direct relation to the movement along the decollement plane. Strikingly, Hilina normal faulting process, responsible for giant landslides and tsunamis, appears to generate no clearly recorded seismic signature, that is, no (or only a few) $M_L > 1$ seismic events. This study therefore cannot bring any direct information concerning the extent of the depth of these scarps: their relative aseismicity can be interpreted as being due to their shallow depth or to the lack of roughness of their surfaces. Recording and studying Hilina related microseismicity probably requires a specific high-sensitivity small-aperture seismic network.

5.2. Southeast Flank of Mauna Loa

[31] Since the Kaoiki (M = 6.6, 16 November 1983) earthquake and the 1984 eruption occurred, Mauna Loa has been moderately active. Earthquake counts and seismicity rates since 1984 remain low, and geodetic data show a pattern of slow and steady reinflation [*Okubo*, 1995]. Geodetic measurements and focal mechanism analyses [e.g., *Bryan and Johnson*, 1991] show that the southeast flank of Mauna Loa is slipping southeastward. The Kaoiki seismogenic zone is located at the interface between the two deforming edifices of Mauna Loa and Kilauea volcanoes.

[32] In the southeast flank of Mauna Loa, 971 of the 5069 events available (i.e., ~20% of the seismicity) have been relocated using cross-spectral time delays (Figures 4c–4e) and 2277 events (i.e., 45% of the seismicity) have been relocated with an average uncertainty of less than 500 m using travel time differences (Figure 5c). Seismicity in the southeast flank of Mauna Loa, especially in its southern part, is more sparse than in the Kilauea south flank and is less favorable to the extensive use of differential techniques, leading to less numerous well-relocated seismic events.

[33] A large number of the events are relocated along a large and gently north dipping subhorizontal structure (Figures 4c–5c) located at a depth of 10–11 km, corresponding probably to the decollement structure already evidenced in the south flank of Kilauea and supposed to be located at the top of the oceanic crust. More remarkably, relative relocations allow us to image a striking feature of Mauna Loa southeast flank seismicity, constituted from a swarm located at a depth of ~7 km in the northern end of Mauna Loa southeast flank. Results of relative relocations for this swarm clearly show a family of three to five subvertical N30° fault planes (Figure 4d). Focal mechanisms coherently show a N30° subvertical solution acting as a right-lateral strike-slip fault (Figure 8). This feature is also present, at the same depth but with fewer events, in the southern part of Mauna Loa southeast flank (Figure 4e): events are relocated along a N45° subvertical fault plane

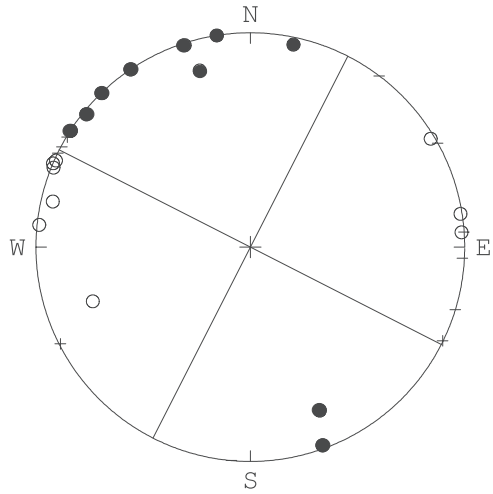

Figure 8. Focal mechanism of one earthquake of the Kaoiki fault zone (Figure 4d).

and also show a right-lateral strike-slip focal mechanism. These events are aligned and share the same focal mechanism; they form a strike-slip zone, ~20 km long and are the probable location for the 1983 Kaoiki M 6.6 earthquake, whose epicenter is located near the northern end of the zone. This strike-slip zone is interpreted as being due to the conjugate action of the magmatic bodies situated at depth below the Kilauea and Mauna Loa volcanoes [*Endo*, 1985; *Wyss et al.*, 1992]. Notice that we confirm, by using accurate relocations, the deformation partition already evidenced by *Wyss et al.* [1992] from stress and strain tensor inversion.

[34] As is proved by the existence of the Kaoiki strike-slip zone, the presence of Kilauea deeply modifies the mechanical behavior of the southeast flank of Mauna Loa. No clear evidence of crustal reverse faulting of any dip was found in the southeast flank of Mauna Loa, though it could be related to Mauna Loa or to Kilauea magmatic storage system. The top of the oceanic crust, inferred from catalog absolute locations of relocated earthquakes (in the hypothesis that subhorizontal seismogenic structures correspond to the top of the oceanic crust), seems to be deeper beneath the Mauna Loa southeast flank than beneath the Kilauea south flank, although this trend could be the result of insufficient station corrections around Mauna Loa. Such a deepening is predicted from plate flexural models [*Thurber and Gripp*, 1988].

6. Conclusion

[35] In this study we investigated 17000 tectonic events of Kilauea and Mauna Loa south flanks and relocated more than 70% with an accuracy in relative positions ranging from 10 to 500 m. Whereas most of these relocated events (80%) are located in the vicinity of subhorizontal decollement planes at a depth of 8–10 km, thought to be the top of the oceanic crust, relocation also revealed steep southeast dipping reverse crustal fault planes beneath this decollement. These reverse crustal fault planes are compatible with the local stress tensor, and are activated during the storage of large quantities of magma at a depth of 3–6 km.

Ruptures in the oceanic floor therefore constitute a major characteristic of the seismicity recorded beneath the south flank of Kilauea. They clearly intersect the decollement plane and could be responsible for the slip-perpendicular alignments of hypocenters imaged by relative relocations on this plane. They are a possible explanation for the remarkable seismicity pattern observed; this pattern can be understood as the expression, in the brittle domain, of a (very slow) strain wave expanding from the volcanic centers as the volcano grows. Crustal reverse faults generate large-scale roughness and normal stress release able to initiate large decollement events beneath the south flank of Kilauea. Finally, steepening of the decollement plane by reverse faulting can induce stresses in the volcanic edifice that may be favorable for initiating Hilina-type instabilities. Crustal reverse faulting therefore provides some coherence in a mechanical model of the growth of Hawaiian volcanoes by explaining various aspects of the deformation pattern observed at different scales in space and time: large-scale seismicity pattern, large earthquake occurrence, Hilina-type instabilities. Rupture of the oceanic floor by reverse faulting is a major characteristics of Kilauea's south flank seismicity, and probably of the Hawaiian volcanoes during a period of their history; it may be an important parameter controlling their growth and topography.

[36] **Acknowledgments.** We (and especially the first author) thank all the USGS HVO staff for their kindness and collaboration, particularly D. Swanson to have accepted J.-L.G. during his 3-month journey at HVO and encouraged and supported this work since its beginning, and all the seismology team (with a special mention to J. Nakata, W. Tanigawa, and K. Honma). We also thank J. Battaglia for his friendly support throughout this study and D. Gillard for his useful advices. We are grateful to A. Rubin, Massimo Cocco, and an anonymous reviewer for their careful reviews. This work was supported by a CRV CNRS grant.

References

Ando, M., The Hawaii earthquake of November 29, 1975: Low dip angle faulting due to forceful injection of magma, *J. Geophys. Res.*, *84*, 7616–7626, 1979.

Bryan, C. J., A possible triggering mechanism for large Hawaiian earthquakes derived from analysis of the June 1989 Kilauea south flank sequence, *Bull. Seismol. Soc. Am.*, *82*, 2368–2390, 1992.

Bryan, C. J., and C. E. Johnson, Block tectonics of the island of Hawaii from a focal mechanism analysis of basal slip, *Bull. Seismol. Soc. Am.*, *81*, 491–507, 1991.

Crosson, R. S., and E. T. Endo, Focal mechanisms of earthquakes related to the 29 November 1975 Kalapana, Hawaii, earthquake: The effect of structure models, *Bull. Seismol. Soc. Am.*, *71*, 713–729, 1981.

Crosson, R. S., and E. T. Endo, Focal mechanisms and locations of earthquakes in the vicinity of the 1975 Kalapana earthquake aftershock zone 1970–1979: Implications for tectonics of the south flank of Kilauea volcano, island of Hawaii, *Tectonics*, *1*, 495–542, 1982.

Delaney, P. T., R. S. Fiske, A. Miklius, and A. T. Okamura, Deep magma body beneath the summit and rift zones of Kilauea Volcano, Hawaii, *Science*, *247*, 1265–1372, 1990.

Dieterich, J. H., Growth and persistence of Hawaiian volcanic rift zones, *J. Geophys. Res.*, *93*, 4258–4270, 1988.

Dieterich, J. H., V. Cayol, and P. G. Okubo, The use of earthquake rate changes as a stress meter at Kilauea volcano, *Nature*, *408*, 457–460, 2000.

Endo, E. T., Seismotectonic framework for the southeast flank of Mauna Loa, Hawaii, Ph.D. thesis, Univ. Of Wash., Seattle, 1985.

Fiske, R. S., and R. Y. Koyanagi, The December 1965 eruption of Kilauea Volcano, Hawaii, *U.S. Geol. Surv. Prof. Pap.*, *607*, 21 pp., 1968.

Furumoto, A. S., and R. L. Kovach, The Kalapana earthquake of November 29, 1975; an intraplate earthquake and its relation to geothermal processes, *Phys. Earth Planet. Inter.*, *18*, 197–208, 1979.

Gillard, D., M. Wyss, and P. G. Okubo, Type of faulting and orientation of stress and strain as a function of space and time in Kilauea's south flank, Hawaii, *J. Geophys. Res.*, *101*, 16,025–16,042, 1996.

Got, J.-L., J. Fréchet, and F. W. Klein, Deep fault plane geometry inferred from multiplet relative relocation beneath the south flank of Kilauea, *J. Geophys. Res.*, *99*, 15,375–15,386, 1994.

Haslinger, F., C. H. Thurber, M. Mandernach, and P. G. Okubo, Tomographic image of *P*-velocity structure beneath Kilauea's East Rift Zone and south flank: Seismic evidence for a deep magma body, *Geophys. Res. Lett.*, *28*, 375–378, 2001.

Hill, D. P., Crustal structure of the island of Hawaii from seismic refraction measurements, *Bull. Seismol. Soc. Am.*, *59*, 101–130, 1969.

Hill, D. P., and J. J. Zucca, Geophysical constraints on the structure of Kilauea and Mauna Loa volcanoes and some implications for seismomagmatic processes, *U.S. Geol. Surv. Prof. Pap.*, *1350*, 903–917, 1987.

Jenkins, G. M., and D. G. Watts, *Spectral Analysis and Its Applications*, Holden-Day, Boca Raton, Fla., 1968.

Kilb, D., and A. M. Rubin, Implications of diverse fault orientations imaged in relocated aftershocks of the Mount Lewis, M_L 5.7, California, earthquake, *J. Geophys. Res.*, *107*(B11), 2294, doi:10.1029/2001JB000149, 2002.

Lipman, P. W., J. P. Lockwood, R. T. Okamura, D. A. Swanson, and K. M. Yamashita, Ground deformation associated with the 1975 magnitude-7.2 earthquake and resulting changes in activity of Kilauea volcano, Hawaii, *U.S. Geol. Surv. Prof. Pap.*, *1276*, 45 pp., 1985.

Okubo, P. G., A seismological framework for Mauna Loa volcano, Hawaii, in *Mauna Loa Revealed: Structure, Composition, History, and Hazards*, *Geophys. Monogr. Ser.*, vol. 92, edited by J. M. Rhodes and J. P. Lockwood, pp. 187–197, AGU, Washington, D. C., 1995.

Okubo, P. G., H. M. Benz, and B. A. Chouet, Imaging the crustal magma sources beneath Mauna Loa and Kilauea volcanoes, Hawaii, *Geology*, *25*, 867–870, 1997.

Rubin, A. M., Using repeating earthquakes to correct high-precision earthquake catalogs for time-dependent station delays, *Bull. Seismol. Soc. Am.*, *92*, 1647–1659, 2002.

Rubin, A. M., D. Gillard, and J.-L. Got, Streaks of microearthquakes along creeping faults, *Nature*, *400*, 635–641, 1999.

Swanson, D. A., W. A. Duffield, and R. S. Fiske, Displacement of the south flank of Kilauea volcano: The result of forceful intrusion of magma into the rift zones, *U.S. Geol. Surv. Prof. Pap.*, *963*, 1–39, 1976.

Thurber, C. H., and A. E. Gripp, Flexure and seismicity beneath the south flank of Kilauea volcano and tectonic implications, *J. Geophys. Res.*, *93*, 4213–4248, 1988.

Waldhauser, F., and W. L. Ellsworth, A double difference earthquake location algorithm: Method and application to the northern Hayward fault, CA, *Bull. Seismol. Soc. Am.*, *90*, 1353–1368, 2000.

Waldhauser, F., W. L. Ellsworth, and A. Cole, Slip-parallel seismic lineations on the northern Hayward fault, California, *Geophys. Res. Lett.*, *26*, 3525–3528, 1999.

Wolfe, C., P. G. Okubo, and P. Shearer, Mantle fault zone beneath Kilauea volcano, Hawaii, *Science*, *300*, 478–480, 2003.

Wyss, M., F. W. Klein, and A. C. Johnston, Precursors to the Kalapana $M = 7.2$ earthquake, *J. Geophys. Res.*, *86*, 3881–3900, 1981.

Wyss, M., B. Liang, W. R. Tanigawa, and X. Wu, Comparison of orientations of stress and strain tensors based on fault plane solutions in Kaoiki, Hawaii, *J. Geophys. Res.*, *97*, 4769–4790, 1992.

Zucca, J. J., and D. P. Hill, Crustal structure of the southeast flank of Kilauea volcano, Hawaii, from seismic refraction measurements, *Bull. Seismol. Soc. Am.*, *70*, 1149–1159, 1980.

Zucca, J. J., D. P. Hill, and R. L. Kovach, Crustal structure of Mauna Loa volcano, Hawaii, from seismic refraction and gravity data, *Bull. Seismol. Soc. Am.*, *72*, 1535–1550, 1982.

J.-L. Got, Laboratoire de Géophysique Interne et Tectonophysique, Université de Savoie, F-73376 Le Bourget-du-Lac, France.

P. Okubo, Hawaiian Volcano Observatory, U.S. Geological Survey, P.O. Box 51, Hawaii National Park, HI 96718, USA. (pokubo@usgs.gov)